

On Interference Dynamics in Matérn Networks

Udo Schilcher, Jorge F. Schmidt, and Christian Bettstetter *Senior Member, IEEE*

Abstract—A thorough understanding of the temporal dynamics of interference in wireless networks is crucial for the design of communication protocols, scheduling, and interference management. This paper applies stochastic geometry to investigate interference dynamics for the first time in a network with nodes that use carrier sense multiple access. This type of networks is approximated by a Matérn hard-core point process of type II with Nakagami fading. We derive and analyze expressions for the variance, covariance, and correlation of the interference power at a given point in space. Results show that even though the commonly used Poisson approximation to carrier sense multiple access may have the same average interference than the Matérn model, the three interference dynamics measurements investigated behave significantly different.

Index Terms—Wireless networks, stochastic geometry, interference, correlation, Matérn point process, hard-core process, Nakagami fading, CSMA.

I. INTRODUCTION

A. Motivation

The modeling and analysis of interference in wireless networks by means of stochastic geometry [1] has become popular in the course of the past 15 years (see [2]–[4]). The majority of work in this domain uses simple modeling assumptions for reasons of mathematical tractability. A common network model includes uniformly randomly distributed nodes employing slotted ALOHA for medium access and Poisson arrival of transmission demands. This leads to uniformly distributed senders for interference analysis, which can be modeled by a Poisson point process (PPP). Such networks are sometimes called *Poisson networks*. They facilitate the derivation of mathematical expressions while retaining important network properties; they are well understood in the communications theory community with several results available in the literature (see [3]–[9]).

In practice, however, many computer and communication networks do not access the shared medium in an ALOHA style but perform some type of *carrier sensing*. A classical example is Carrier Sense Multiple Access (CSMA), in which each node senses the medium and only starts to send a message if the medium is idle (otherwise backs off according to some rule and tries to send at a later instant) with the goal to reduce the number of message collisions. CSMA is also the basis for medium access control in IEEE 802.11 [10]. Although such medium sensing is not captured by Poisson networks, CSMA networks are approximated in most analytical studies by Poisson networks [11]–[15]. This approximation has been shown to be accurate for first-order statistics of the interference

power, i.e., statistics on interference at one point in space, such as expected value and variance (see [12], [13], [16]). Its suitability for higher-order statistics of the interference (i.e., at several points in time or space) is, however, still unknown.

A better, very natural choice to model senders with carrier sensing is a Matérn hard-core point process (MPP) [17]. It introduces a guard circle around each sender, in which no node is allowed to send [3], [18]. This resembles the medium sensing and is suited for any kind of wireless network with spatial reservation of a transmission floor. Such *Matérn networks* are still only approximations for CSMA networks because real CSMA protocol implementations are more complex. For example, there is a chance that two close nodes send simultaneously due to imperfect sensing or hidden node effects. MPP assumes perfect sensing, thus leading to a slight underestimation of interference. Nevertheless, the approximation by MPP is much closer to CSMA than any PPP model and brings the theory of interference calculus a step forward in the direction of more realistic models. From a more general perspective, only few analytical results are available for MPPs, severely limiting the accurate analysis of many modern wireless technologies. The paper at hand intends to fill this research gap with special emphasis on the stochastic analysis of interference dynamics.

B. Contributions

We derive expressions for the expected value, variance, covariance, and temporal correlation of the interference power at an arbitrary point in space in a network with carrier sensing modeled by an MPP of type II. Wireless links are modeled by a distance-dependent path loss and Nakagami small-scale fading. The derived expressions are analyzed to highlight the pitfalls of the popular Poisson approximation to CSMA and to explore the impact of system parameters on the correlation of interference. The main novelty is that **expressions for higher-order moments and correlation of interference have been unknown so far for Matérn networks**. These measures show as to how interference changes over time: Is it changing strongly or weakly (variance)? Is it changing quickly or slowly (correlation)? Along these lines, our results give a deeper and more realistic understanding of the *temporal dynamics of interference* in wireless networks.

From a practical perspective, such understanding is useful in the design of communication protocols, scheduling, and interference management for many popular wireless technologies for which only rough approximations are available today. A cooperative relaying protocol, for example, should take into account the correlation of interference to choose its relay. For instance, a higher correlation requires a higher number of potential relays [19]. Furthermore, LTE Release

Udo Schilcher is with Lakeside Labs GmbH, Klagenfurt, Austria, E-Mail: schilcher@lakeside-labs.com. Jorge F. Schmidt, and Christian Bettstetter are with the Institute of Networked and Embedded Systems, University of Klagenfurt, Austria, E-mail: {jorge.schmidt, christian.bettstetter}@aau.at.

13 specifies a licensed-assisted access (LAA) operation mode, that includes a listen-before-talk channel sensing mechanism to support coexistence with WiFi in the unlicensed spectrum (see [20], [21]). LAA is also perceived to be a key feature of 5G networks [22].

Our scientific contributions can be summarized as follows:

- We derive expressions for the probabilities of one or two points in a PPP being retained in one or two independent Matérn thinnings of the PPP.
- We derive expressions for the expected value, variance, covariance, and temporal correlation of interference in Matérn networks.
- We show that interference correlation in Matérn networks is significantly different from that in Poisson networks, which leads to the qualitative conclusion that a PPP is unsuited to capture second-order properties of CSMA networks.
- We analyze the dependence of the interference correlation on the system parameters and show that, in contrast to Poisson networks, it depends on the intensity of the MPP and the path loss exponent. Furthermore, fading has a stronger impact on the correlation in networks with carrier sensing.

C. Related Work

Related work mainly includes publications on the modeling of CSMA networks by means of stochastic point processes and publications on interference dynamics in wireless networks. Let us first revisit some work on the use of MPPs in the analysis of interference. The mean interference experienced by a node can be calculated by numerical integration [18]; also an upper bound in terms of a closed-form expression is available [23]. Considering network performance, a coverage analysis using a PPP approximation is done in [3], which is then used to calculate the sensing sensitivity that maximizes the density of concurrent transmissions. Furthermore, the mean throughput [24] and the capacity in case of high SIR [25] have been calculated. All these results have in common that they only consider first-order statistics to analyze the network, i.e., they analyze interference at a single point in time and space. Hence, these results are incapable of capture the dynamic change of interference. In contrast, we aim to quantify the dynamics of interference (in terms of temporal correlation), which is essential to evaluate a wide range of communication methods, e.g., diversity techniques [6] and MIMO in millimeter wave communications [26].

Networks with carrier sensing are also modeled with soft-core point processes [27]–[29]. Unlike hard-core point processes, there is no strict minimum distance between senders. Instead, a repelling force between senders is assumed that is stronger if they are closer. Hence, it is unlikely for two senders to be very close to each other, yet it is not impossible. This resembles a form of imperfect carrier sensing [27]. Although soft-core processes are probably even more realistic models for CSMA networks, they are rarely applied due to the lack of analytical results.

Alternative models for CSMA networks include perturbed triangular lattices [30] and SSI processes [31]. These alternatives are investigated almost exclusively by simulations with almost no analytical results available.

The temporal and spatial correlation of interference is studied in [8], [9], [19], [32] but with restriction to PPPs.

The paper is structured as follows: Section 2 explains the modeling assumptions, including node placement, wireless channel, and interference. Section 3 derives expressions for the mean value, variance, covariance, and correlation of interference under this model. Section 4 analyzes the interference correlation and compares results to those of a Poisson network. Section 5 concludes.

II. NETWORK MODEL

A. Spatial Distribution of Senders

The potential senders in a wireless network are distributed according to a PPP $\Phi_p \subset \mathbb{R}^2$ with intensity λ_p . Time is partitioned into slots of equal duration. In each slot t , some of the potential senders act as senders, i.e., they transmit some data. These senders are modeled by an MPP of type II, denoted by $\Phi \subseteq \Phi_p$. Note that we do not consider the receivers; they are neither included in Φ nor in Φ_p . Instead, we assume that each sender has an associated receiver within its range similar to the Poisson bipolar network model ([33], [34]).

The decision of a potential sender about sending in a slot t is based on a sensing mechanism for medium access. This mechanism should prevent two nodes from simultaneously sending if their distance is below a certain threshold d , which is similar to CSMA [3]. This behavior is modeled, in each slot, by a dependent thinning of Φ_p , resulting in an MPP of type II with intensity λ for the senders. In other words, the selection of senders is done independently per slot by performing a Matérn thinning of a PPP in each slot.

Such Matérn type II thinning works as follows [1]: Each node $x \in \Phi_p$ draws a uniformly i.i.d. random mark $m_x \sim \mathcal{U}(0, 1)$. Node x is retained if and only if m_x is smaller than the marks m_y of all points $y \in \mathcal{C}(x, d)$, where $\mathcal{C}(x, r) = \{y \in \mathbb{R}^2 \mid \|x - y\| \leq r\}$ is a circle with radius r centered at x .

The mechanism is fair in the sense that all potential senders are treated equally due to the stationarity of the MPP. It needs to be mentioned that, in real CSMA networks, there is still a possibility that nodes arbitrarily close to each other start sending simultaneously due to imperfect sensing. This effect is not covered by the Matérn model and is outside the scope of this work.

B. Wireless Channel

The radio propagation is modeled by distance-dependent path loss and small-scale fading caused by multipath propagation. All nodes transmit with unit power. The power p received at the origin o from a sender x is given by $p = h_x^2 \ell(\|x\|)$. The term $\ell(\|x\|) = \min(1, \|x\|^{-\alpha})$ is the distance-dependent path gain with exponent $\alpha > 2$. The random variable h_x^2 models small-scale fading. We employ the versatile Nakagami- m fading model [35], for which the random variable h_x^2 follows

a gamma distribution with parameter m , i.e., $h_x^2 \sim \Gamma(m, \frac{1}{m})$ with mean $\mathbb{E}[h_x^2] = 1$. Recall that the Nakagami model also covers Rayleigh fading ($m = 1$) and no fading ($m \rightarrow \infty$).

C. Interference

We are interested in the overall interference at an arbitrary location. Due to the stationarity of the point processes we consider, without loss of generality, interference at the origin o . This model could be applied for a scenario in which the node suffering from the interference is not an inherent part of the network that causes it. An example application could be mmWave base stations within a 5G cellular network [36] that are interfered by the cellular system without being part of it.

The interference power at time t_i (time index i) is calculated as the sum of the signal powers arriving at the origin o from all active senders, i.e.,

$$\begin{aligned} I_i &= \sum_{x \in \Phi_p} h_x^2 \ell(\|x\|) \gamma_x(t_i) \\ &= \sum_{x \in \Phi(t_i)} h_x^2 \ell(\|x\|), \end{aligned} \quad (1)$$

where $\gamma_x(t_i)$ is the indicator function that a point x is retained by Matérn thinning at time t_i , i.e., that it sends in slot t_i .

III. INTERFERENCE EXPRESSIONS

Our overall goal is to derive the temporal correlation of interference in a given point in space in a Matérn network in terms of Pearson's correlation coefficient $\rho[I_1, I_2]$. As a basic ingredient for the correlation, we start by calculating the probabilities of a point being retained by the Matérn thinning.

A. Retainment Probabilities

Let p_1 and p_{12} denote the probability that a point is retained once and twice, respectively, and $p_{1/1}(r)$ and $p_{1/2}(r)$ denote the probability that two different points at distance r are retained in one and in two thinnings, respectively.

Lemma 1 (Single point is retained once): The probability that a point $x \in \Phi_p$ is retained by Matérn thinning is [1]

$$p_1 = \frac{1 - \exp(-\lambda_p d^2 \pi)}{\lambda_p d^2 \pi}, \quad (2)$$

where $d^2 \pi$ is the area of a circle with radius d representing the sensing area of a node.

Proof (for didactic purposes): For a given mark m_x of $x \in \Phi_p$ with $0 \leq m_x \leq 1$ the point process $\Phi_t = \{y \in \Phi_p \mid m_y < m_x\}$ is an independent m_x -thinning of Φ_p . Hence, it is itself a PPP with intensity $m_x \lambda_p$. A point $x \in \Phi_p$ is retained in the Matérn thinning if $\Phi_t \cap b(x, d) = \emptyset$. Thus, the retainment probability for a given m_x is the void probability $\exp(-m_x \lambda_p d^2 \pi)$. Since the mark m_x is chosen by x uniformly in $[0, 1]$, the probability that x is retained in the Matérn thinning is

$$p_1 = \int_0^1 \exp(-m_x \lambda_p d^2 \pi) dm_x. \quad (3)$$

Solving this integration yields the result. ■

Remarks:

- From this Lemma it immediately follows that [1]

$$\lambda = \lambda_p p_1 = \frac{1 - \exp(-\lambda_p d^2 \pi)}{d^2 \pi}. \quad (4)$$

- The theoretical maximum intensity of an MPP for a given d is $\lim_{\lambda_p \rightarrow \infty} \lambda = \frac{1}{d^2 \pi}$. Every node possesses an empty guard area of $d^2 \pi$. This point process is sometimes criticized for having low intensities [31], but it can actually achieve λ up to this limit if one chooses a large enough PPP intensity λ_p .
- For $d \rightarrow \infty$ the probability that a point is retained vanishes, i.e., $\lim_{d \rightarrow \infty} p_1 = 0$. For $d \rightarrow 0$ all points are retained, i.e., $\lim_{d \rightarrow 0} p_1 = 1$.

Lemma 2 (Single point is retained twice): The probability that a point $x \in \Phi_p$ is retained twice by two independent Matérn thinnings is

$$p_{12} = \frac{\exp(-\lambda d^2 \pi) (E_i(\lambda d^2 \pi) - \log(\lambda d^2 \pi) - \gamma_{\text{eul}})}{\lambda d^2 \pi}, \quad (5)$$

where $E_i(x)$ denotes the exponential integral function and $\gamma_{\text{eul}} \approx 0.577216$ denotes Euler's γ constant.

Proof: This proof goes along the lines of the proof of Lemma 1. Let $m_{x,1}$ and $m_{x,2}$ with $0 \leq m_{x,1}, m_{x,2} \leq 1$ denote the marks of $x \in \Phi_p$ in the first and the second thinning, respectively. We consider the point process $\Phi_{t^2} = \{y \in \Phi_p \mid m_{y,1} < m_{x,1} \vee m_{y,2} < m_{x,2}\}$ of all points having a mark being smaller than $m_{x,1}$ in the first or smaller than $m_{x,2}$ in the second thinning. The probability that an arbitrary point is in this set is $m_{x,1} + m_{x,2} - m_{x,1} m_{x,2}$ by the inclusion-exclusion principle. Hence, the point process Φ_{t^2} has the intensity $(m_{x,1} + m_{x,2} - m_{x,1} m_{x,2}) \lambda$. The probability that no point of Φ_{t^2} is located in $b(x, d)$ is then given by the void probability of the process Φ_{t^2} , i.e., by $\exp(- (m_{x,1} + m_{x,2} - m_{x,1} m_{x,2}) \lambda d^2 \pi)$. Therefore, the probability that x is retained twice is

$$p_{12} = \int_0^1 \int_0^1 e^{-(m_{x,1} + m_{x,2} - m_{x,1} m_{x,2}) \lambda d^2 \pi} dm_{x,1} dm_{x,2}. \quad (6)$$

Solving these integrals yields the result. ■

Remarks:

- The probability p_{12} that a given point x is retained twice is not the retaining probability squared, i.e., $p_{12} \neq p_1^2$ for all $d > 0$. The reason is that the number of neighboring points that are potential "killers" of x is different for any $x \in \Phi_p$ but stays constant over time. Hence, the retainings of x in different thinnings are correlated.
- We have $p_{12} > p_1^2$ for all $d > 0$, i.e., a point that is retained once is more likely to be retained a second time. This fact can be explained by the following intuition: A point x that is retained once has, on average, fewer neighboring points that could have potentially killed x . Therefore, in another independent thinning it has higher chances of being retained. In the limit, the probabilities converge to $\lim_{d \rightarrow \infty} p_1 = \lim_{d \rightarrow \infty} p_{12} = 0$.
- The intensity of points that are retained twice is given by $\lambda_p p_{12}$.

- For $d \rightarrow 0$ all points are retained twice in two independent thinnings, i.e., $\lim_{d \rightarrow 0} p_{12} = 1$.

Lemma 3 (Two distinct points are retained in one thinning):

The probability that two points separated by a distance r are both retained in a Matérn thinning is given by [1]

$$p_{1/1}(r) = \frac{2\Gamma_d(r)(1 - \exp(-\lambda d^2\pi))}{\lambda^2 d^2 \pi \Gamma_d(r)(\Gamma_d(r) - d^2\pi)} - \frac{2(1 - \exp(-\lambda \Gamma_d(r)))}{\lambda^2 \Gamma_d(r)(\Gamma_d(r) - d^2\pi)} \quad (7)$$

for $r > d$ and 0 otherwise. Here, $\Gamma_d(r)$ is the area covered by two overlapping circles with radius d and centers separated by r , which is given by

$$\Gamma_d(r) = 2d^2\pi - \gamma_d(r). \quad (8)$$

The overlapping area of these two circles is

$$\gamma_d(r) = 2d^2 \arccos\left(\frac{r}{2d}\right) - \frac{r}{2} \sqrt{4d^2 - r^2} \quad (9)$$

for $r \leq 2d$ and 0 otherwise [1].

Proof: Let us consider two points $x, y \in \Phi_p$ at distance $\|x - y\| = r > 0$. If $r \leq d$, it is impossible that both points are retained due to the definition of a hard-core point process. Hence, let $r > d$ in the following. Recall that whether x and y are retained depends on the marks of the points in $\mathcal{C}(x, d)$ and $\mathcal{C}(y, d)$, respectively. If $r < 2d$, these circles overlap and we subdivide them into three areas: $A_c := \mathcal{C}(x, d) \cap \mathcal{C}(y, d)$ is the common area, $A_x := \mathcal{C}(x, d) \setminus \mathcal{C}(y, d)$ and $A_y := \mathcal{C}(y, d) \setminus \mathcal{C}(x, d)$ are the non-common areas. The sizes of these areas are [1]

$$|A_c| = \gamma_d(r) \stackrel{r \leq 2d}{=} 2d^2 \arccos\left(\frac{r}{2d}\right) - \frac{r}{2} \sqrt{4d^2 - r^2} \quad (10)$$

$$|A_x| = |A_y| = d^2\pi - \gamma_d(r). \quad (11)$$

For $r \geq 2d$ the common area vanishes giving $|A_c| = 0$. The area covered by at least one of the circles is

$$|A_x \cup A_y| = \Gamma_d(r) = 2d^2\pi - \gamma_d(r). \quad (12)$$

Let m_x and m_y denote the marks of x and y , respectively. To retain both x and y , the following three conditions have to hold: Firstly, A_x must not contain any point from $z \in \Phi_p$ with $m_z < m_x$. For given m_x , the probability for it is $\exp(-m_x \lambda_p |A_x|)$, similarly to the proofs of Lemma 1 and 2. Secondly, A_y must not contain any $z \in \Phi_p$ with $m_z < m_y$, which happens with probability $\exp(-m_y \lambda_p |A_y|)$. Thirdly, the common area A_c must not contain any $z \in \Phi_p$ with $m_z < \max(m_x, m_y)$, which has the probability $\exp(-\max(m_x, m_y) \lambda_p |A_c|)$. Overall, the probability that both x and y are retained is

$$p_{1/1}(r) = \int_0^1 \int_0^1 \exp\left(- (m_x + m_y) \lambda_p |A_x| - \max(m_x, m_y) \lambda_p |A_c|\right) dm_x dm_y. \quad (13)$$

Solving these integrals yields the result. ■

Remarks:

- Based on the probability in (7), we can calculate the second-order product density of the MPP by $\rho^{(2)}(r) = \lambda_p^2 p_{1/1}(r)$. A plot of it is shown in Fig. 1.

- For the case $r > 2d$ we have $\gamma_d(r) = 0$ and hence $\rho^{(2)}(r) = \lambda^2$, since $p_{1/1}(r) \stackrel{r \geq 2d}{=} p_1^2$. This implies that two points that are further than $2d$ apart from each other are independently retained or removed. Recall that the second-order product density for PPPs is λ_p^2 .
- For the case $d < r \leq 2d$ the integration over $\rho^{(2)}(r)$ yields no closed form solution due to the complexity of $\gamma_d(r)$. Hence, in some cases it might be advantageous to approximate it by $\gamma_d(r) \approx d^2\pi - 2dr$ [1].

Lemma 4 (Two distinct points are retained in independent thinnings): The probability $p_{1/2}(r)$ that a point $x \in \Phi_p$ is retained by a thinning and $y \in \Phi_p$ is retained in another, independent thinning with $r = \|x - y\| > 0$ is given in (14) for $r \geq d$ and in (15) for $r < d$.

Proof: Let us consider two points $x, y \in \Phi_p$ at distance $\|x - y\| = r > 0$. We define the areas A_c, A_x and A_y as given in (10) and (11) of the proof of Lemma 3.

Let us assume $r > d$. For given m_x and m_y , there should be no point $z \in \Phi_p$ with $m_z < m_x$ in the area A_x at the first thinning and no point $z \in \Phi_p$ with $m_z < m_y$ in A_y at the second thinning. The probability for these events is given by

$$\exp\left(- (m_x + m_y) \lambda_p (d^2\pi - \gamma_d(r))\right). \quad (16)$$

The probability that there is no point $z \in \Phi_p$ in A_c with $m_z < m_x$ at the first or $m_z < m_y$ at the second thinning is

$$\exp\left(- (m_x + m_y - m_x m_y) \lambda_p \gamma_d(r)\right) \quad (17)$$

similar to the proof of Lemma 2. Integrating over the product of these two expressions yields

$$p_{1/2}(r) \stackrel{r \geq d}{=} \int_0^1 \int_0^1 \exp\left(- (m_x + m_y) \lambda_p (d^2\pi - \gamma_d(r)) - (m_x + m_y - m_x m_y) \lambda_p \gamma_d(r)\right) dm_x dm_y. \quad (18)$$

Next, we assume that $r < d$. In this case, the derivation of $p_{1/2}(r)$ is similar to the previous case, except $x \in A_c$ in the first thinning and $y \in A_c$ in the second one. Hence, x has to have a higher mark than y in the first thinning, and y a higher mark than x in the second thinning. These two events have the probabilities $(1 - m_x)$ and $(1 - m_y)$ respectively, leading to

$$p_{1/2}(r) \stackrel{r \leq d}{=} \int_0^1 \int_0^1 \exp\left(- (m_x + m_y) \lambda_p (d^2\pi - \gamma_d(r)) - (m_x + m_y - m_x m_y) \lambda_p \gamma_d(r)\right) (1 - m_x)(1 - m_y) dm_x dm_y. \quad (19)$$

Solving the integrations in (18) and (19) yields the result. ■

Remarks:

- The probability $p_{1/1}(r)$ vanishes for $r < d$ since two points closer than d cannot both be retained in one thinning. However, the probability that each of them is retained in an independent thinning is $p_{1/2}(r) > 0$ for $r < d$. Still, it is much smaller than for $r \geq d$ (see Fig. 1), since for $r \geq d$ they are neighbors and could potentially kill each other, i.e., the random number of neighbors is higher by one in this case.

$$p_{1/2}(r) \stackrel{r \geq d}{=} \frac{\exp\left(-\frac{d^4 \pi^2 \lambda_p}{\gamma_d(r)}\right) \left(2\Gamma\left(0, d^2 \pi \lambda_p \left(1 - \frac{d^2 \pi}{\gamma_d(r)}\right)\right) - \Gamma\left(0, -\frac{d^4 \pi^2 \lambda_p}{\gamma_d(r)}\right) - \Gamma\left(0, -\frac{\lambda_p (\gamma_d(r) - d^2 \pi)^2}{\gamma_d(r)}\right)\right)}{\lambda_p \gamma_d(r)} \quad (14)$$

$$p_{1/2}(r) \stackrel{r \leq d}{=} \frac{\exp\left(-d^2 \pi \lambda_p \left(2 + \frac{d^2 \pi}{\gamma_d(r)}\right)\right)}{d^2 \pi \lambda_p^2 \gamma_d^3(r)} \left(\exp(2d^2 \pi \lambda_p) \left(\gamma_d(r) (1 + 2d^2 \pi \lambda_p - \gamma_d(r) \lambda_p) - d^4 \pi^2 \lambda_p\right) \right. \\ \left. \left(2E_i\left(d^2 \pi \lambda_p \left(\frac{d^2 \pi}{\gamma_d(r)} - 1\right)\right) - E_i\left(\frac{d^4 \pi^2 \lambda_p}{\gamma_d(r)}\right) - E_i\left(\frac{\lambda_p (\gamma_d(r) - d^2 \pi)^2}{\gamma_d(r)}\right)\right) \right. \\ \left. - \gamma_d(r) \exp\left(\frac{d^4 \pi^2 \lambda_p}{\gamma_d(r)}\right) \left(\exp(\lambda_p \gamma_d(r)) d^2 \pi + \exp(2d^2 \pi \lambda_p) (d^2 \pi - 2\gamma_d(r)) - 2 \exp(d^2 \pi \lambda_p) (d^2 \pi - \gamma_d(r))\right) \right) \quad (15)$$

- If the two points approach each other and become identical, the probability $p_{1/2}(r)$ becomes the probability p_{12} that one point is retained twice, i.e., $\lim_{r \rightarrow 0} p_{1/2}(r) = p_{12}$. Care has to be taken when calculating this limit: We have to adopt (14), which is intended for $r \geq d$ and does not consider an extra point in the neighborhood. Hence, in the limit when the two points merge to become one, there is no extra point in the neighborhood leading to (5). Calculating the limit of (15) leads to the different expression $\frac{\exp(-\lambda d^2 \pi) (1 + E_i(\lambda d^2 \pi) - \log(\lambda d^2 \pi) - \gamma_{\text{eul}}) - 1}{\lambda d^2 \pi}$.
- If $r > 2d$, the events that two points are retained each in an independent thinning are independent. Therefore, we have $p_{1/2}(r) \stackrel{r > 2d}{=} p_1^2$.

Note that for $d \rightarrow 0$ all results in this section converge to the corresponding results of a PPP.

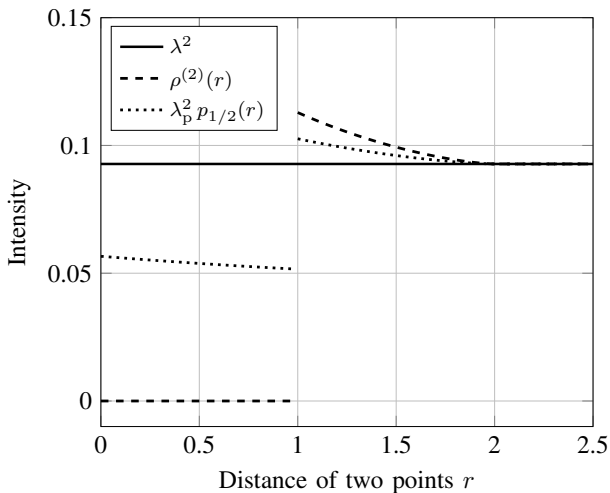


Fig. 1. Intensity of the MPP λ^2 (not a function of r), of two points separated by r retained in the same thinning $\rho^{(2)}(r)$ (the second-order product density), and of two points separated by r each retained in an independent thinning $\lambda_p^2 p_{1/2}(r)$. Parameters are $\lambda_p = 1$ and $d = 1$.

B. Expected Value, Variance, and Covariance of Interference

Lemma 5 (Expected interference): The expected value of interference is

$$\mathbb{E}[I] = \lambda \frac{\alpha \pi}{\alpha - 2}. \quad (20)$$

Proof: All nodes in the set $\Phi \subseteq \Phi_p$ are considered to be interferers. Hence, the expected value of interference is calculated by applying Campbell's theorem yielding

$$\mathbb{E}[I] = \mathbb{E} \left[\sum_{x \in \Phi_p} h_x^2 \ell(\|x\|) \gamma_x(t) \right] \quad (21) \\ = \lambda_p \int_{\mathbb{R}^2} \ell(\|x\|) \mathbb{E}[h_x^2] \mathbb{E}[\gamma_x(t)] dx \\ = \lambda_p p_1 \frac{\alpha \pi}{\alpha - 2}.$$

The expected value of the indicator function $\gamma_x(t)$ does neither depend on x nor on t . This is because we do not consider any nodes to be placed at certain locations (e.g., the origin), which implies that we do not adopt the Palm distribution of the MPP. Substituting (4) into this expression gives the result. ■

Remarks:

- The expected interference (20) for MPP is the same as the one for PPP (given in [4], [37]) with the same process intensity using the same path loss model.
- The expression (20) does not correspond to the expected interference derived by Haenggi for MPP [18]. The core difference is in the modeling assumptions: Haenggi assumes that a node is located at the origin; his result thus represents the expected interference experienced by a typical node in the network. This assumption causes some mathematical difficulties, as the reduced Palm distribution has to be adopted. We do not assume a node to be located at the origin; all results hold for any point in space. Nevertheless, a data sink could be located at this point that neither sends data nor participates in the CSMA protocol. Along these lines, our assumptions are well-suited for a multipoint-to-point communication scenario.

Theorem 1 (Variance of interference): The variance of interference at the origin o is

$$\begin{aligned} \text{var}[I] &= \lambda \frac{(m+1)\alpha\pi}{m(\alpha-1)} \\ &+ 8\pi \int_{\frac{d}{2}}^{\infty} \int_0^{\infty} \int_0^{2\pi} \ell(r(\cosh \mu + \cos \nu)) \\ &\ell(r(\cosh \mu - \cos \nu)) \frac{r^2}{2} (\cosh 2\mu - \cos 2\nu) d\nu d\mu \\ &\rho^{(2)}(2r) r dr - \left(\frac{\lambda\alpha\pi}{\alpha-1} \right)^2, \end{aligned} \quad (22)$$

where λ is the intensity of the MPP, m is the parameter of Nakagami fading, α is the path loss exponent, d is the hard-core distance, and $\ell(\cdot)$ is the path gain function.

Proof: We start by calculating the second moment of interference at time t by

$$\begin{aligned} \mathbb{E}[I^2] &= \\ &= \mathbb{E} \left[\left(\sum_{x \in \Phi_p} h_x^2 \ell(\|x\|) \gamma_x(t) \right) \right. \\ &\quad \left. \cdot \left(\sum_{y \in \Phi_p} h_y^2 \ell(\|y\|) \gamma_y(t) \right) \right] \\ &\stackrel{(a)}{=} \mathbb{E} \left[\sum_{x \in \Phi_p} (h_x^2 \ell(\|x\|))^2 \gamma_x(t) \right] \\ &\quad + \mathbb{E} \left[\sum_{x, y \in \Phi_p}^{\neq} h_x^2 \ell(\|x\|) h_y^2 \ell(\|y\|) \gamma_x(t) \gamma_y(t) \right], \end{aligned} \quad (23)$$

where in (a) terms with $x = y$ are separated from terms with $x \neq y$. The first of these expected values yields

$$\begin{aligned} \mathbb{E} \left[\sum_{x \in \Phi_p} (h_x^2 \ell(\|x\|))^2 \gamma_x(t) \right] &= \\ &\stackrel{(a)}{=} \lambda_p p_1 \mathbb{E}[h_x^4] \int_{\mathbb{R}^2} \ell^2(\|x\|) dx \\ &= \lambda \frac{(m+1)\alpha\pi}{m(\alpha-1)}, \end{aligned} \quad (24)$$

where in (a) we apply Campbell's theorem. The last expectation of (23) gives

$$\begin{aligned} \mathbb{E} \left[\sum_{x, y \in \Phi_p}^{\neq} h_x^2 \ell(\|x\|) h_y^2 \ell(\|y\|) \gamma_x(t) \gamma_y(t) \right] &= \\ &\stackrel{(a)}{=} \int_{\mathbb{R}^2} \int_{\mathbb{R}^2} \ell(\|x\|) \ell(\|y\|) \rho^{(2)}(\|x-y\|) dx dy \\ &\stackrel{(b)}{=} 4 \int_{\mathbb{R}^2} \int_{\mathbb{R}^2} \ell(\|x\|) \ell(\|x-2a\|) \rho^{(2)}(\|2a\|) dx da \\ &\stackrel{(c)}{=} 4 \int_{\mathbb{R}^2} \int_{\mathbb{R}^2} \ell(\|x+a\|) \ell(\|x-a\|) dx \rho^{(2)}(\|2a\|) da \\ &\stackrel{(d)}{=} 8\pi \int_{\frac{d}{2}}^{\infty} \int_{\mathbb{R}^2} \ell \left(\left\| x + \begin{pmatrix} r \\ 0 \end{pmatrix} \right\| \right) \ell \left(\left\| x - \begin{pmatrix} r \\ 0 \end{pmatrix} \right\| \right) dx \\ &\rho^{(2)}(2r) r dr. \end{aligned} \quad (25)$$

In (a) we apply a basic property of the second-order product density $\rho^{(2)}(r) = \lambda_p^2 p_{1/1}(r)$ [1, p. 112], where $p_{1/1}(r)$ is the probability that two points at distance r are both retained, as derived in Lemma 3. Furthermore, the expected values of the fading coefficients $\mathbb{E}[h_z^2] = 1$ for any $z \in \Phi_p$ are substituted. In (b) we substitute $y = x - 2a$, and 4 is the corresponding Jacobi determinant; in (c) we substitute $x + a$ for x . In (d) we substitute polar coordinates. The integration of r starts at $\frac{d}{2}$ as $\rho^{(2)}(r) = 0$ for $r < d$. Furthermore, we apply a rotation of the coordinate system to translate a into a real number a' :

$$\mathbf{x}' = \begin{pmatrix} \cos \phi & \sin \phi \\ -\sin \phi & \cos \phi \end{pmatrix} \mathbf{x}, \quad (26)$$

where \mathbf{x}' and \mathbf{x} are the vector notations of points x' and x in \mathbb{R}^2 , respectively, and $\phi = \arctan(a_I/a_R)$ is the phase of the polar coordinate of a . This transformation does not change the norms $\ell(\|x+a\|)$, $\ell(\|x-a\|)$, and $\ell(\|2a\|)$ involved in the integration. This can be verified by writing $x' = e^{j\phi}x$ and $a' = e^{j\phi}a$.

For an arbitrary but fixed $r \in \mathbb{R}$, the inner integral of (25) is

$$\begin{aligned} \int_{\mathbb{R}^2} \ell(\|x+a\|) \ell(\|x-a\|) dx &= \\ &\stackrel{(a)}{=} \int_0^{\infty} \int_0^{2\pi} \ell(r(\cosh \mu + \cos \nu)) \\ &\ell(r(\cosh \mu - \cos \nu)) \frac{r^2}{2} (\cosh 2\mu - \cos 2\nu) d\nu d\mu. \end{aligned} \quad (27)$$

In (a) we substitute elliptic coordinates defined as

$$\begin{aligned} x_1 &= r \cosh \mu \cos \nu \\ x_2 &= r \sinh \mu \sin \nu \end{aligned} \quad (28)$$

and its corresponding Jacobi determinant $\frac{r^2}{2} (\cosh 2\mu - \cos 2\nu)$, and calculate the corresponding norms. Calculating $\text{var}[I] = \mathbb{E}[I^2] - \mathbb{E}[I]^2$ yields the result. ■

Remarks:

- The variance of interference is presented in terms of integral expressions that are solved numerically as there is no closed-form solution. The problematic term for symbolic integration is the second-order product density $\rho^{(2)}(r)$.
- Since numerical integration is involved in calculating the variance of interference some steps of the proof would not be needed. For example, the expression in step (a) of (25) could directly be solved numerically. However, it turns out that it is advantageous to rather solve the integration in (22) as it results in better numerical stability.
- The substitution of elliptic coordinates might be an interesting approach for other applications: It allows to solve integrations of the form $\int_{\mathbb{R}^2} \|x-a\| \|x+a\| dx$, which sometimes occur in the derivation of second order statistics of interference for both PPP and MPP.
- When $d \rightarrow 0$ the variance converges to the Poisson case: In (25) (a) the second-order product density $\rho^{(2)}(r)$ could be substituted by λ^2 leading to

$$\mathbb{E} \left[\sum_{x, y \in \Phi_p}^{\neq} h_x^2 \ell(\|x\|) h_y^2 \ell(\|y\|) \gamma_x(t) \gamma_y(t) \right] = (29)$$

$$\begin{aligned}
&= \left(\lambda \int_{\mathbb{R}^2} \ell(\|x\|) dx \right)^2 \\
&= \left(\lambda \frac{\alpha\pi}{\alpha-2} \right)^2.
\end{aligned}$$

Since this expression is equal to $\mathbb{E}[I]^2$, we have

$$\text{var}[I] = \lambda \frac{(m+1)\alpha\pi}{m(\alpha-1)} \quad (30)$$

equal to the Poisson case [8].

Theorem 2 (Covariance of interference): The temporal covariance of interference at the origin o is

$$\begin{aligned}
\text{cov}[I_1, I_2] &= \lambda_p p_{12} \frac{\alpha\pi}{\alpha-1} \\
&+ 8\pi \int_0^\infty \int_0^\infty \int_0^{2\pi} \ell(r(\cosh\mu + \cos\nu)) \\
&\ell(r(\cosh\mu - \cos\nu)) \frac{r^2}{2} (\cosh 2\mu - \cos 2\nu) d\nu d\mu \\
&p_{1/2}(2r) r dr - \left(\frac{\lambda\alpha\pi}{\alpha-2} \right)^2,
\end{aligned} \quad (31)$$

where λ_p is the intensity of the PPP, $\lambda = \lambda_p p_1$ is the intensity of the MPP, m is the parameter of Nakagami fading, α is the path loss exponent, d is the hard-core distance, and $\ell(\cdot)$ is the path gain function. $p_{1/2}(r)$ denotes the probability that two different nodes are retained in two independent Matérn thinnings, as derived in Lemma 4.

Proof: The proof goes along the lines of the proof of Theorem 1. We start by calculating the covariance of interference at times t_1 and t_2 by

$$\begin{aligned}
\mathbb{E}[I_1 I_2] &= \\
&= \mathbb{E} \left[\left(\sum_{x \in \Phi_p} h_x^2 \ell(\|x\|) \gamma_x(t_1) \right) \right. \\
&\quad \left. \cdot \left(\sum_{y \in \Phi_p} h_y^2 \ell(\|y\|) \gamma_y(t_2) \right) \right] \\
&\stackrel{(a)}{=} \mathbb{E} \left[\sum_{x \in \Phi_p} \ell^2(\|x\|) \gamma_x(t_1) \gamma_x(t_2) \right] \\
&\quad + \mathbb{E} \left[\sum_{x, y \in \Phi_p}^{\neq} \ell(\|x\|) \ell(\|y\|) \gamma_x(t_1) \gamma_y(t_2) \right],
\end{aligned} \quad (32)$$

where in (a) terms with $x = y$ are separated from terms with $x \neq y$ and the expected value of fading $\mathbb{E}[h_x^2] = 1$ is substituted. The first of these expected values yields

$$\begin{aligned}
\mathbb{E} \left[\sum_{x \in \Phi_p} \ell^2(\|x\|) \gamma_x(t_1) \gamma_x(t_2) \right] &= \\
&\stackrel{(a)}{=} \lambda_p p_{12} \int_{\mathbb{R}^2} \ell^2(\|x\|) dx \\
&= \lambda_p p_{12} \frac{\alpha\pi}{\alpha-1},
\end{aligned} \quad (33)$$

where in (a) we apply Campbell's theorem. The second expectation of (32) gives

$$\begin{aligned}
\mathbb{E} \left[\sum_{x, y \in \Phi_p}^{\neq} h_x^2 \ell(\|x\|) h_y^2 \ell(\|y\|) \gamma_x(t_1) \gamma_y(t_2) \right] &= \\
&\stackrel{(a)}{=} \lambda_p^2 \int_{\mathbb{R}^2} \int_{\mathbb{R}^2} \ell(\|x\|) \ell(\|y\|) p_{1/2}(\|x-y\|) dx dy.
\end{aligned} \quad (34)$$

In (a) we apply a basic property of the process, where $p_{1/2}(r)$ is the probability that two points at distance r are both retained each in an independent Matérn thinning, as derived in Lemma 4. Note that this expression is similar to (23) except that the second-order product density $\rho^{(2)}(2r)$ is substituted by $\lambda_p^2 p_{1/2}(2r)$. Applying similar steps as in the proof of Theorem 1 yields the result. ■

Remarks:

- The covariance does not depend on fading as there is no m in the expression.
- Again, for $d \rightarrow 0$ the expression of $\text{cov}[I_1, I_2]$ converges to the Poisson case: As mentioned in the remarks after Lemma 4, we have $p_{1/2}(r) \stackrel{r > 2d}{\approx} p_1^2$. Substituting this result into (34) leads to

$$\begin{aligned}
\mathbb{E} \left[\sum_{x, y \in \Phi_p}^{\neq} h_x^2 \ell(\|x\|) h_y^2 \ell(\|y\|) \gamma_x(t_1) \gamma_y(t_2) \right] &= \\
&= \left(\lambda \int_{\mathbb{R}^2} \ell(\|x\|) dx \right)^2,
\end{aligned} \quad (35)$$

which is equal to $\mathbb{E}[I]^2$. Thus, we have

$$\text{cov}[I_1, I_2] = \lambda_p p_{12} \frac{\alpha\pi}{\alpha-1}. \quad (37)$$

C. Correlation of Interference

Corollary 1 (Correlation of interference): The temporal correlation of interference $\rho[I_1, I_2]$ at the origin o is given in (38).

Proof: Pearson's correlation coefficient is defined as $\rho[I_1, I_2] = \frac{\text{cov}[I_1, I_2]}{\sqrt{\text{var}[I_1] \text{var}[I_2]}}$. Hence, the result is obtained by dividing (31) by (22). ■

Remarks:

- In the limit $d \rightarrow 0$ the temporal correlation of interference approaches the Poisson case with all potential senders transmitting:

$$\lim_{d \rightarrow 0} \rho[I_1, I_2] = \frac{m}{m+1}. \quad (39)$$

In particular, for Rayleigh fading ($m = 1$) the correlation is $\lim_{d \rightarrow 0} \rho[I_1, I_2] \stackrel{m=1}{=} \frac{1}{2}$ and without fading we have $\lim_{m \rightarrow \infty} \lim_{d \rightarrow 0} \rho[I_1, I_2] = 1$.

- The temporal correlation of interference does not depend on the time period between I_i and I_j . In other words, for a given time instant t , the correlation $\rho[I_t, I_{t+i}]$ is the same for all $i \in \mathbb{Z}$. This result is relevant for retransmission protocols: If a transmission failed and has to be repeated, the sender can expect the same interference statistics independent of the time instant of the retransmission, i.e., a longer backoff does not increase the success probability in this model.

$$\rho[I_1, I_2] = \frac{\frac{\lambda(m+1)\alpha\pi}{m(\alpha-1)} + 8\pi \int_{\frac{d}{2}}^{\infty} \int_0^{\infty} \int_0^{2\pi} \frac{\ell(r(\cosh \mu + \cos \nu))\ell(r(\cosh \mu - \cos \nu))r^2(\cosh 2\mu - \cos 2\nu)}{2} d\nu d\mu \rho^{(2)}(2r)r dr - \left(\frac{\lambda\alpha\pi}{\alpha-2}\right)^2}{\frac{\lambda_p p_{12} \alpha \pi}{\alpha-1} + 8\pi \int_0^{\infty} \int_0^{\infty} \int_0^{2\pi} \frac{\ell(r(\cosh \mu + \cos \nu))\ell(r(\cosh \mu - \cos \nu))r^2(\cosh 2\mu - \cos 2\nu)}{2} d\nu d\mu p_{1/2}(2r)r dr - \left(\frac{\lambda\alpha\pi}{\alpha-2}\right)^2}. \quad (38)$$

IV. INSIGHTS ON INTERFERENCE CORRELATION

So far we have derived expressions for the MPP and explained how these are generalizations of the PPP. Let us now plot and analyze the interference correlation of the Matérn network over certain parameters and compare these results to those of a Poisson network. For a fair comparison, the senders in the Poisson network are selected by an independent thinning of the PPP with probability p_1 , leading to an intensity λ (which is the density of senders in the Matérn network). This model resembles ALOHA as MAC protocol, where the sending probability is p_1 . Both the CSMA and the ALOHA network model have the same expected value of interference $\mathbb{E}[I]$. Remember that, unlike for PPPs, conditioning on a point at the origin o does change the distribution of the rest of the process for MPPs, since there cannot be any point in its vicinity, i.e., $\mathcal{C}(o, d) \cap \Phi \setminus \{o\} = \emptyset$. In this work, we do not condition on having a point of the process being located at the origin o .

If not stated otherwise, we use a path loss exponent $\alpha = 3$ and an intensity $\lambda_p = 1$ for the PPP, hence having $0 \leq \lambda \leq 1$, depending on the value of d . The hard-core distance is $d = 1$.

All mathematical results have been crosschecked by simulations, showing a good match. All plots show only the mathematical results because the simulation results do not provide any additional information.

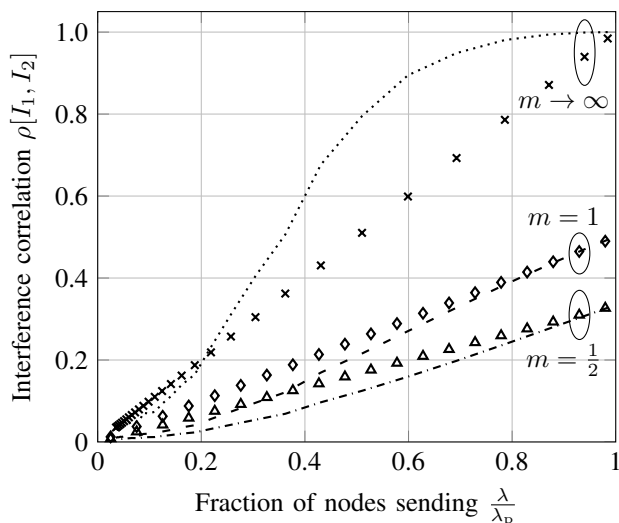


Fig. 2. Temporal correlation of interference over different densities of transmitters. Lines indicate MPP and marks indicate PPP. Parameters are $\lambda_p = 1$ and $\alpha = 3$.

A. Impact of Fraction of Sending Nodes

Fig. 2 shows the temporal correlation of interference for different fractions of nodes acting as interferers for both PPP

and MPP. For the MPP, this correlation is calculated by numerical integration of the expression in Corollary 1 and is plotted over p_1 given in (2), varying the value of d . For the PPP, the scenario corresponds to Case (2, 1, 1) in the classification of [32]; the correlation is $\frac{q^m}{m+1}$ with q being the fraction of active senders [8], [32].

The most apparent observation is that PPP and MPP yield significantly different correlation curves. Hence, adopting a PPP to model a CSMA network may lead to the correct average interference, but it will incorrectly estimate the temporal dynamics in terms of correlation. Nevertheless, the curves of both models show the same trend: The correlations are strictly monotonically increasing with the fraction of senders and hit the same maximum value of $\frac{m}{m+1}$ for $\lambda \rightarrow \lambda_p$, i.e., $p_1 \rightarrow 1$. In particular, the interference correlation of a PPP is neither an upper nor a lower bound for the one of an MPP. In general, it is higher for a small fraction of senders and lower for a high fraction. The crossing point heavily depends on the fading: weak fading (high m) shifts the crossing point toward small fractions of senders.

B. Impact of Fading

Fig. 3 shows how the interference correlation depends on the severeness of fading represented by m . It is well known for PPPs that the correlation of interference decreases with increasing fading (decreasing m). The reason is that severe fading leads to a high variance of interference but does not change the covariance. We observe the same qualitative behavior for MPPs. All curves flatten out for increasing m , and in case of no fading ($m \rightarrow \infty$), the correlation converges to a value that depends on λ and d , which is plotted in Fig. 2 (dotted curve). The value of m determines as to which of the two models shows a higher correlation. Last but not least, the curves show that severe fading (small m) has higher impact on the correlation of MPPs than of PPPs.

Fig. 4 shows that the interference correlation in the MPP depends on the path loss exponent α , while it is independent of α for PPPs. This dependence is, however, very small: For low α (close to 2), the correlation is slightly smaller than for higher values. For values $\alpha \geq 3$, there is almost no change in correlation when further increasing α .

C. Impact of Sensing Range

Fig. 5 shows that the interference correlation decreases with increasing hard-core distance d and eventually vanishes for $d \rightarrow \infty$. The reason for this behavior is that d determines the number of senders. A higher d models a more sensitive sensing, which implies fewer simultaneously sending nodes that are further apart. If a higher fraction of nodes send, naturally the temporal correlation is higher, and vice versa.

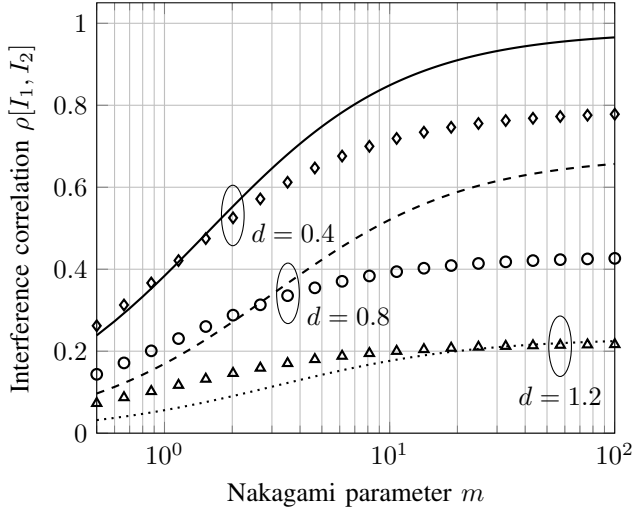


Fig. 3. Temporal correlation of interference over different values of the fading parameter m . Lines indicate MPP and marks indicate PPP. Parameters are $\lambda_p = 1$ and $\alpha = 3$.

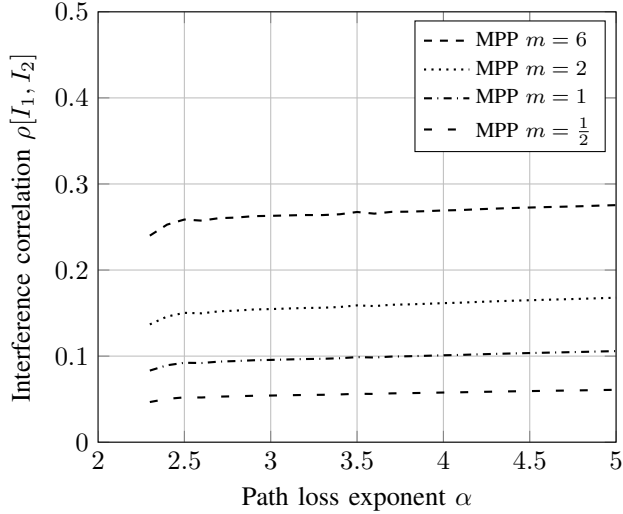


Fig. 4. Temporal correlation of interference over different values of the path loss exponent α . Parameters are $\lambda_p = 1$ and $d = 1$. Numerical integrations are unstable for $\alpha < 2.3$.

This is already known for PPPs with a linear relation between fraction of senders and correlation [8]. For MPPs, we have the same qualitative behavior but with a non-linear relation between fraction of senders and correlation.

Overall, we conclude that sensing sensitivity determines the interference correlation: If the sensing is very sensitive, few nodes are sending, thus the correlation is small. If the sensing is nonsensitive, correlation increases up to the point where there is no sensing, which eventually yields slotted ALOHA. In mathematical terms, this is modeled by $d \rightarrow 0$ leading to a PPP.

D. Impact of Intensity

Fig. 6 plots the interference correlation of a Matérn network over the intensity λ_p of the PPP from which the MPP is derived from. It shows a strong decrease of correlation for

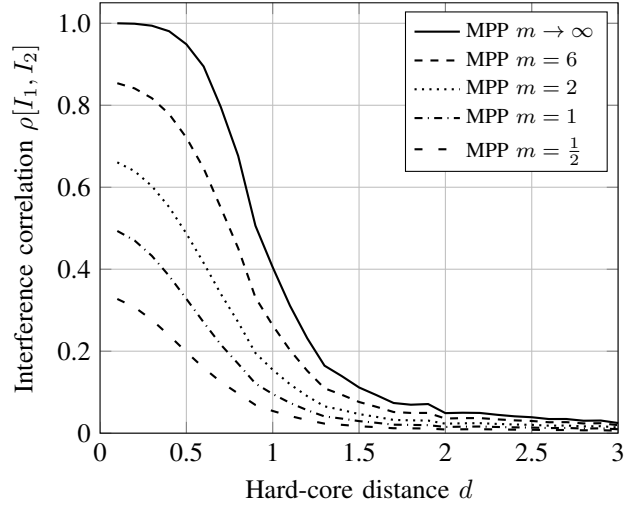


Fig. 5. Temporal correlation of interference over different values of the hard-core distance d . Parameters are $\lambda_p = 1$ and $\alpha = 3$. The glitches in the curves (e.g., close to $d = 2$) are due to instabilities in numerical integrations.

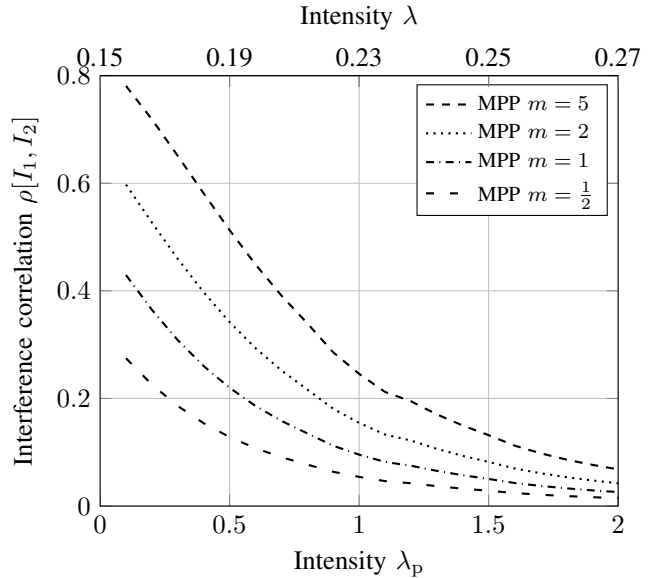


Fig. 6. Temporal correlation of interference over different values of the intensity λ_p of the PPP to which Matérn thinning is applied. Parameters are $d = 1$ and $\alpha = 3$. The upper axis label shows the intensity λ of the MPP. It monotonically increases with λ_p and is upper bounded by $\frac{1}{d^2\pi}$.

increasing λ_p . This is in contrast to Poisson networks, where the intensity has no impact on interference correlation. The main reason for this dependency in MPPs is that d does not scale with λ_p . Hence, for a higher density, a smaller fraction of nodes is allowed to send, since they are on average closer packed, which reduces the retainment probability p_1 . Indeed, from (2), we can conclude that p_1 monotonically decreases with increasing λ_p .

V. CONCLUSIONS

This article contributes to interference calculus in wireless networks with emphasis on the dynamics of interference in Matérn networks with Nakagami fading. We derived and

analyzed previously unknown expressions for the variance and covariance of interference power and calculated the correlation coefficient.

We proved that the interference dynamics is significantly different in networks with carrier sensing than in networks without sensing. An important difference is that the interference correlation in Matérn networks depends on the intensity of the underlying point process, which is irrelevant in Poisson networks. The path loss exponent has almost no influence on interference correlation in both types of networks. These results demonstrate the limits of the commonly used Poisson network model. At the same time, our results highlight the potential of the Matérn point process as a viable model for networks with carrier sensing; it approximates important aspects of CSMA while remaining tractable to a certain extent.

ACKNOWLEDGMENTS

This work has been supported by the Austrian Science Fund (FWF) under grant P24480-N15 (Dynamics of Interference in Wireless Networks). It has also been supported by the K-project DeSSnet, which funded within the context of COMET – Competence Centers for Excellent Technologies by the Austrian Ministry for Transport, Innovation and Technology (BMVIT), the Federal Ministry for Digital and Economic Affairs (BMDW), and the federal states of Styria and Carinthia. The program is conducted by the Austrian Research Promotion Agency (FFG).

REFERENCES

- [1] D. Stoyan, W. S. Kendall, and J. Mecke, *Stochastic Geometry and Its Applications*. John Wiley & Sons Ltd, 1995.
- [2] M. Haenggi, J. G. Andrews, F. Baccelli, O. Dousse, and M. Franceschetti, “Stochastic geometry and random graphs for the analysis and design of wireless networks,” *IEEE Journal on Selected Areas in Communications*, vol. 27, pp. 1029–1046, Sept. 2009.
- [3] F. Baccelli and B. Błaszczyszyn, *Stochastic Geometry and Wireless Networks, Volume II: Applications*. now publishing, 2009.
- [4] M. Haenggi, *Stochastic Geometry for Wireless Networks*. Cambridge University Press, 2013.
- [5] U. Schilcher, S. Toumpis, M. Haenggi, A. Crismani, G. Brandner, and C. Bettstetter, “Interference functionals in Poisson networks,” *IEEE Trans. Inf. Theory*, vol. 62, pp. 370–383, Jan. 2016.
- [6] M. Haenggi and R. Smarandache, “Diversity polynomials for the analysis of temporal correlations in wireless networks,” *IEEE Trans. Wireless Commun.*, vol. 12, pp. 5940–5951, Nov. 2013.
- [7] U. Schilcher, S. Toumpis, A. Crismani, G. Brandner, and C. Bettstetter, “How does interference dynamics influence packet delivery in cooperative relaying?,” in *Proc. ACM/IEEE Intern. Conf. on Modeling, Analysis and Simulation of Wireless and Mobile Systems (MSWiM)*, Nov. 2013.
- [8] R. Ganti and M. Haenggi, “Spatial and temporal correlation of the interference in ALOHA ad hoc networks,” *IEEE Commun. Lett.*, vol. 13, pp. 631–633, Sept. 2009.
- [9] R. Tanbourgi, H. S. Dhillon, J. G. Andrews, and F. K. Jondral, “Effect of spatial interference correlation on the performance of maximum ratio combining,” *IEEE Trans. Wireless Commun.*, vol. 13, pp. 3307–3316, June 2014.
- [10] “IEEE standard for information technology: Telecommunications and information exchange between systems local and metropolitan area networks: Specific requirements - part II: Wireless LAN medium access control (MAC) and physical layer (PHY) specifications,” *IEEE Std 802.11-2016*, Dec. 2016.
- [11] B. Kaufman, J. Lilleberg, and B. Aazhang, “Spectrum sharing scheme between cellular users and ad-hoc device-to-device users,” *IEEE Trans. Wireless Commun.*, vol. 12, no. 3, pp. 1038–1049, 2013.
- [12] Q. Ye, M. Al-Shalash, C. Caramanis, and J. G. Andrews, “Resource optimization in device-to-device cellular systems using time-frequency hopping,” *IEEE Trans. Wireless Commun.*, pp. 5467–5480, 2013.
- [13] H. ElSawy, E. Hossain, and M.-S. Alouini, “Analytical modeling of mode selection and power control for underlay D2D communication in cellular networks,” *IEEE Trans. Commun.*, vol. 62, pp. 4147–4161, Nov 2014.
- [14] X. Lin, J. G. Andrews, and A. Ghosh, “Spectrum sharing for device-to-device communication in cellular networks,” *IEEE Trans. Wireless Commun.*, vol. 13, no. 12, pp. 6727–6740, 2014.
- [15] J. F. Schmidt, M. K. Atiq, U. Schilcher, and C. Bettstetter, “Underlay device-to-device communications in LTE-A: Uplink or downlink?,” in *Proc. IEEE Int. Symp. on Personal, Indoor and Mobile Radio Commun. (PIMRC)*, pp. 1692–1696, 2015.
- [16] H. Q. Nguyen, F. Baccelli, and D. Kofman, “A stochastic geometry analysis of dense IEEE 802.11 networks,” in *Proc. IEEE INFOCOM*, pp. 1199–1207, May 2007.
- [17] B. Matérn, *Spatial Variation*. Springer Lecture Notes in Statistics, 1986.
- [18] M. Haenggi, “Mean interference in hard-core wireless networks,” *IEEE Commun. Lett.*, vol. 15, pp. 792–794, Aug. 2011.
- [19] A. Crismani, S. Toumpis, U. Schilcher, G. Brandner, and C. Bettstetter, “Cooperative relaying under spatially and temporally correlated interference,” *IEEE Trans. Veh. Technol.*, vol. 64, pp. 4655–4669, Oct. 2015.
- [20] “Feasibility study on licensed-assisted access to unlicensed spectrum,” *3GPP TR 36.889 v13.0.0*, July 2015.
- [21] H. J. Kwon, J. Jeon, A. Borkar, Q. Ye, H. Harada, Y. Jiang, L. Liu, S. Nagata, B. L. Ng, T. Novlan, J. Oh, and W. Yi, “Licensed-assisted access to unlicensed spectrum in LTE release 13,” *IEEE Commun. Mag.*, vol. 55, pp. 201–207, Feb. 2017.
- [22] A. Mukherjee, J. F. Cheng, S. Falahati, H. Koorapaty, D. H. Kang, R. Karaki, L. Falconetti, and D. Larsson, “Licensed-assisted access LTE: coexistence with IEEE 802.11 and the evolution toward 5G,” *IEEE Commun. Mag.*, vol. 54, pp. 50–57, June 2016.
- [23] B. Cho, K. Koufos, and R. Jantti, “Bounding the mean interference in Matérn type II hard-core wireless networks,” *IEEE Commun. Lett.*, vol. 2, pp. 563–566, Oct. 2013.
- [24] H. Q. Nguyen, F. Baccelli, and D. Kofman, “A stochastic geometry analysis of dense IEEE 802.11 networks,” in *Proc. IEEE Intern. Conf. on Computer Commun. (INFOCOM)*, pp. 1199–1207, May 2007.
- [25] R. K. Ganti, J. G. Andrews, and M. Haenggi, “High-SIR transmission capacity of wireless networks with general fading and node distribution,” *IEEE Trans. Inf. Theory*, vol. 57, pp. 3100–3116, May 2011.
- [26] J. G. Andrews, T. Bai, M. N. Kulkarni, A. Alkhatieb, A. K. Gupta, and R. W. Heath, “Modeling and analyzing millimeter wave cellular systems,” *IEEE Trans. Commun.*, vol. 65, pp. 403–430, Jan. 2017.
- [27] N. Deng, W. Zhou, and M. Haenggi, “The Ginibre point process as a model for wireless networks with repulsion,” *IEEE Trans. Wireless Commun.*, vol. 14, pp. 107–121, Jan. 2015.
- [28] D. B. Taylor, H. S. Dhillon, T. D. Novlan, and J. G. Andrews, “Pairwise interaction processes for modeling cellular network topology,” in *Proc. IEEE Global Commun. Conf. (GLOBECOM)*, Dec. 2012.
- [29] G. L. Torrisi and E. Leonardi, “Large deviations of the interference in the Ginibre network model,” *Stoch. Syst.*, vol. 4, pp. 173–205, 2014.
- [30] F. Lagum, S. S. Szyszkowicz, and H. Yanikomeroglu, “Quantifying the regularity of perturbed triangular lattices using CoV-based metrics for modeling the locations of base stations in HetNets,” in *Proc. IEEE Vehic. Techn. Conf. (VTC-Fall)*, Sept. 2016.
- [31] A. Busson and G. Chelius, “Point processes for interference modeling in CSMA/CA ad-hoc networks,” in *Proc. ACM Symp. on Performance Eval. of Wireless Ad Hoc, Sensor, and Ubiquitous Netw. (PE-WASUN)*, (New York, NY, USA), pp. 33–40, Oct. 2009.
- [32] U. Schilcher, C. Bettstetter, and G. Brandner, “Temporal correlation of interference in wireless networks with Rayleigh fading,” *IEEE Trans. Mobile Comput.*, vol. 11, pp. 2109–2120, Dec. 2012.
- [33] M. Haenggi, “The meta distribution of the SIR in poisson bipolar and cellular networks,” *IEEE Trans. Wireless Commun.*, vol. 15, pp. 2577–2589, Apr. 2016.
- [34] F. Baccelli, B. Błaszczyszyn, and P. Muhlethaler, “An ALOHA protocol for multihop mobile wireless networks,” *IEEE Trans. Inf. Theory*, vol. 52, pp. 421–436, Feb. 2006.
- [35] M. Nakagami, “The m -distribution — a general formula of intensity distribution of rapid fading,” in *Proc. Statistical Methods in Radio Wave Propagation*, (Los Angeles, CA, USA), pp. 3–36, June 1958.
- [36] M. Shafi, A. F. Molisch, P. J. Smith, T. Haustein, P. Zhu, P. D. Silva, F. Tufvesson, A. Benjebbour, and G. Wunder, “5G: A tutorial overview of standards, trials, challenges, deployment, and practice,” *IEEE J. Sel. Areas Commun.*, vol. 35, pp. 1201–1221, June 2017.
- [37] U. Schilcher, C. Bettstetter, and G. Brandner, “Temporal correlation of interference in wireless networks with Rayleigh block fading,” *IEEE Trans. Mobile Comput.*, vol. 11, pp. 2109–2120, Dec. 2012.



Udo Schilcher studied applied computing and mathematics at the University of Klagenfurt, where he received two Dipl.-Ing. degrees with distinction (2005, 2006). From 2005 to 2017, he was research staff member at the Institute of Networked and Embedded Systems at the University of Klagenfurt. His doctoral thesis on inhomogeneous node distributions and interference correlation in wireless networks and has been awarded with a Dr. techn. degree with distinction in 2011. After his graduation, from 2011 he was Post-Doc, again at the Institute of Networked and Embedded Systems at the University of Klagenfurt. Since 2016 he has been senior researcher at Lakeside Labs GmbH. His main interests are interference dynamics and spatial node distributions in wireless networks, and stochastic geometry. He received a best paper award from the IEEE Vehicular Technology Society.



Jorge F. Schmidt received the B.Sc. and D.Sc. degrees in electrical engineering from the Universidad Nacional del Sur, Bahía Blanca, Argentina, in 2005 and 2011, respectively. From 2012 to 2014, he was a Postdoctoral Fellow in the Signal Processing and Communications Laboratory at the University of Vigo, Spain. In 2014 he joined the Institute of Networked and Embedded Systems group at University of Klagenfurt, Austria, where he is currently a Senior Researcher. Since 2016 he is also a Senior Researcher at Lakeside Labs GmbH, Austria. His main research interests lie in the area of statistical signal processing and interference modeling and management for wireless communications systems. He received a best paper award from the ACM SIGSIM.



Christian Bettstetter (S'98-M'04-SM'09) received the Dipl.-Ing. degree in 1998 and the Dr.-Ing. degree (summa cum laude) in 2004, both in electrical and information engineering from Technische Universität München (TUM), Munich, Germany. He was a research and teaching staff member at the Institute of Communication Networks, TUM, until 2003. From 2003 to 2005, he was a senior researcher with DOCOMO Euro-Labs. He has been a professor at the University of Klagenfurt, Austria, since 2005, and founding director of the Institute of Networked and Embedded Systems since 2007. He is also the founding scientific director of Lakeside Labs, a research company on self-organizing networked systems.